Journal of Modern Processes in Manufacturing and Production, Volume 9, No. 2, Spring 2020

DOR: 20.1001.1.27170314.2020.9.2.4.8

Research Paper

Effect of Electrical Potential on the Morphology of Polyvinyl Alcohol/ Sodium Alginate Electrospun Nanofibers, Containing Herbal Extracts of Calendula Officinalis for Using in Biomedical Applications

Seyed Rasoul Tahami[1], Nahid Hassanzadeh Nemati[1*], Hamid Keshvari[2], Mohammad Taghi Khorasani[3]

[1]Department of Biomedical Engineering, Science and Research Branch, Islamic Azad University, Tehran, Iran

[2]Department of Biomedical Engineering, Amirkabir University of Technology (Tehran Polytechnic), Tehran, Iran

[3]Department of Biomaterial, Iran Polymer and Petrochemical Institute, Tehran, Iran

*Email of Corresponding Author: nahid_hasanzadeh@yahoo.com, hasanzadeh@srbiau.ac.ir

Received: April 20, 2020; Accepted: June 22, 2020

Abstract

This study aimed to investigate the effect of electrical potential on the morphology of Polyvinyl Alcohol/Sodium Alginate electrospun nanofibers, containing herbal extracts of Calendula Officinalis. For this purpose, Poly Vinyl Alcohol (PVA)/ Sodium Alginate (SAlg) nanofibers were prepared using the electrospinning method in aqueous solutions with PVA (8% w / v)/SAlg (2% w / v) blended system in a volume ratio of 80/20. Then Calendula officinalis extract (10% w / v)in a volume ratio of 10% of PVA/SAlg blended system added. Applying potentials were 5, 10, 15, and 20 kV. The electrospun fibers were characterized by scanning electron microscopy (SEM). The results show that all the produced mats had high-porosity and high-surface to volume ratio of electrospun fibers. In all applied potentials, the diameter of the nanofibers containing Calendula was more than the Calendula-free Nanofibers. On the other hand, the diameters of the Nanofibers in each sample decreased with enhancing the potential. Without significant changes in mat morphology, PVA/SAlg electrospun nanofibers diameter including the Calendula could be controlled with electrical potential in electrospinning. The results could be used in antibacterial meshes, wound dressings, drug delivery, and tissue engineering applications.

Keywords

Calendula Officinalis, Electrospinning, Nanofibers, Polyvinyl Alcohol, Sodium Alginate

1. Introduction

Since the mid-1990s, there has been a growing interest in the production of nanofibres by electrospinning. It is a simple and cost-effective process carried out at room temperature that allows the production of polymer fibers with diameters in the sub-micron size range, through the application of an external electric field, keeping intact the bulk properties of the polymer [1, 2]. In a typical electrospinning process, an electrostatic force is applied to overcome the surface tension of a charged liquid which normally comes out of a syringe with a metallic needle connected to a high-

voltage power supply. The electrostatic force stretches or breaks up the charged liquid to be viscoelastic filaments or jets, resulting finally in dry fibrous or particulate polymeric products after the evaporation of the solvent in the liquid during the journey towards a grounded fiber or particle collector. A broad range of materials can be processed by electrospinning. The morphology and structure (diameter, surface morphology, interior structure, etc.) and properties of electrospun products can be effectively controlled, which makes electrospinning very promising for a variety of applications, ranging from the energy field to biomedical and healthcare applications [3].

The polymer is dissolved in the solvent and then loaded into a syringe with a needle attached. The syringe containing the solution is then placed into the syringe pump with the high voltage probe attached at the needle. As the voltage is applied, the droplet of polymer solution at the needle tip will deform above a threshold voltage into a conical shape, often referred to as a Taylor cone, from which a jet will be extruded towards a target at a lower potential [4]. At very low concentrations, fabricated particles collapse into rings, discs, etc., by varying the electrospraying condition. By increasing the concentration, spherical particles can be formed with different sizes by changing the flow rate and applied voltage. Further, the increase in concentration results in the formation of particle-tail structures or beaded fibers depending on the processing condition. When a critical concentration is reached, uniform fibers are produced. Although these general principles are applicable for most electrospinning/ electrospraying conditions, solutions with specific properties such as high conductivity may behave differently [5, 6].

Sodium alginate (SAlg) probably has the largest number of applications in biomedical science and bioengineering because of its biocompatibility, biosorption, and ease of gelation. Alginate is typically used in the form of a hydrogel in biomedicine, including wound healing, drug delivery, and tissue engineering applications [7]. Alginates are at present still exclusively extracted from algal sources although production by microbial fermentation is technically feasible. The most important feature of alginate's physical properties is the selective binding of multivalent cations, which is the basis for gel formation, a direct mixing of alginate and multivalent cations rarely produces homogeneous gels due to the very rapid and irreversible binding of such ions. Alginates have for many years been used as devices in various human health applications, such as excipients in drug delivery (DDS), wound dressings, as dental impression materials, and in some formulations preventing gastric reflux [8]. Alginate is a naturally hydrophilic and anionic polymer with carboxylic groups, which is typically obtained from brown seaweed after being modified with alkaline aqueous solutions [9].

Polyvinyl alcohol (PVA) is a water-soluble material containing large amounts of hydroxide groups that have been developed for biomedical applications since it is biocompatible and nontoxic, and exhibits minimal cell adhesion [10]. PVA is a linear polymer obtained by vinyl acetate polymerization, followed by partial (70%) or full (100%) hydrolysis. The molar mass of the different types of PVA varies from 10.000 $g \cdot mol^{-1}$-1 to 190.000 $g \cdot mol^{-1}$ [11]. Due to their simple structure and unique properties such as adhesiveness, strength, film-forming, biocompatibility, swelling, safety, and non-carcinogenicity, PVA polymers have found applications in different industries including textiles, paper, adhesives, food, biomedical and pharmaceutical in particular [12, 13].

Due to its low cost, low toxicity, biocompatibility, and biodegradability, alginate, and PVA have been extensively studied for biomedical applications. PVA/SAlg electrospun nanofibers have promising biomedical applications in different fields .In a study by Yang et al., 3T3 cells were cultured on PVA/SAlg electrospun fibers, showed good cell viability. The usage of PVA/SAlg electrospun fiber as scaffold may be appropriate for tissue engineering [14]. Shalumon et al. reported that PVA/SAlgelectrospun nanofibers with the optimal concentration of ZnO could be ideal for wound dressing applications, also, these mats showed good potential for L929 fibroblast cell adhesion [15]. In another study by Tang et al. [16], SA/PVAnanofibrous membranes exhibited smooth and uniform mats and they showed that cytotoxicity assay could be a candidate for wound dressing. Kataria et al. [17] used the electrospinning technique to develop ciprofloxacin loaded transdermal patch from PVA/NAlg nanofibers to deliver control delivery of the drug to wound. And it was shown Higuchi and Korsmeyer–Peppas model for drug release. Therefore, based on the work done, these nanofibers were identified as appropriate for the local delivery of drug at control.

Calendula officinalis (pot marigold) is an annual plant species of Mediterranean origin, popularly used in wound healing and as an anti-inflammatory agent [18]. Calendula Officinalis, commonly known as Marigold, has been traditionally used for its anti-inflammatory effects. Extracts of it have also been found to have anti-oxidant, anti-fungal, anti-edema, anti-diabetic and wound healing properties. The major constituents of Calendula Officinalis include steroids, terpenoids, triterpenoids, flavonoids, phenolic acids, and carotenes. Faradiol, rutin, caffeic acid, and chlorogenic acid have all been isolated from Calendula Officinalis and have shown biological activity in the body. The most potent anti-inflammatory effects of Calendula have been attributed to the faradiol monoesters. Faradiol belongs to the triterpenoid family and has shown anti-inflammatory effects similar to indomethacin, a non-steroidal anti-inflammatory, at an equimolar dose. Rutin, one of the major flavonoids found in many vegetable materials, has also been associated with anti-inflammatory effects as well as anti-bacterial, and hepatoprotective activity. Synthetic derivatives of rutin such as troxerutin are also medically used to strengthen blood vessels. Caffeic acid, a phenolic compound, and its ester chlorogenic acid are commonly associated with anti-oxidant activities [19].

In this study, a blend of aqueous SAlg/PVAand aqueous SAlg/ PVA containing aqueous extract of Calendula officinalis at different voltages was investigated to study the effect of voltage on the mats and the obtained fibers. The structural similarity of the obtained fibers with the extracellular matrix could be suitable for biological applications, especially wound dressing and tissue engineering.

2. Materials and Methods

SAlg from the Sigma Aldrich, PVA from Merck (Hydrolysis degree: > 98%, molecular weight: 72000 Dalton), Calendula officinalis extract [10.7% (w/v) - Series number: CAO-HA – 97016] was purchased from Ebnemasouyeh pharmaceutical Co. All materials were used without further purification.

2.1 Preparation of PVA/SAlg Blend Solutions

Firstly, PVA and SAlg were dissolved separately. SAlg 2% (w-v) was dissolved in distilled water at room temperature with continuous stirring for 3–4 h. Transparent solutions of PVA 8% (w / v) and

was prepared by dissolving PVA in distilled water at about 80 ◦C with continuous stirring for 6 h. Secondly, the PVA solution was mixed with SAlg solution to obtain the blends with the volume ratios of PVA to SAlg ranging 80/20 (PVA/SAlg). Each blended solution was stirred for 6 h at room temperature. In the end, Calendula officinalis (CA) solution [10/7%(W/V)] was mixed with a blend of PVA/SAlgto obtain the solution with the volume ratios of the Officinalis to PVA/SAlg ranging 10/90(PVA /SAlg/CA10%) [20-22].

2.2 Electrospinning of PVA/SAlg and PVA /SAlg/CA10% Blend Nanofibers

The needle is fed with feed solutions (PVA/SAlg solution and PVA /SAlg/CA10% solution, separately in two different stages) from a syringe mounted on a programmable syringe pump. An aluminum foil wrapped on a rotating cylinder was used as the grounded collector. A syringe pump was used to control the flow rate at 0.5 ml/hr. A constant tip to collector distance 15 cm was maintained in all the experiments [23]. Electrospinning was performed by applying variable voltages at 5, 10, 15, and 20 kV, respectively, For each of the samples. All the solutions and fiber samples were stored at room temperature. The diameter and morphology of the fibers collected were determined using a scanning electron microscope (SEM) [24], (AIS-2100 model, Seron Technology, South Korean) after gold coating by a sputter coater (SC7620 model, Emitech, UK). The fiber diameter was measured from the field-emission SEM images, and five images were used for each fiber sample. At least 20 different fibers were randomly selected from each image and their diameter was measured to obtain the average fiber diameter.

During electrospinning, the PVA/SAlg and PVA /SAlg/CA10% solutions in a syringe via an alligator clip attached to the syringe needle for applying a high-voltage at a range from 5 to 20 kV. The solution was delivered to the blunt needle tip via a syringe pump for controlling the solution flow rate. Fibers were collected on electrically grounded aluminum foil placed at a 15 cm distance to the needle tip.

3. Results and Discussion

Specifically, to form fibers, the applied voltage should be sufficient to overcome the surface tension at the tip of the Taylor cone, to initiate the ejection of the charged jet [25]. In this study, the solutions of PVA/SAlg and PVA /SAlg/CA10% were electrospun under the applied voltages of 5, 10, 15, and 20 kV over a tip-to-target distance of 15 cm. The fibers were obtained from both solution under 10, 15 and 20 kV, were continuous and uniform, whereas no fiber deposition was seen from the solutions at the 5 kV Because the voltage applied to the tip of the cone Taylor was not enough to overcome the surface tension to initiate driving the charged jet (Figure 1).

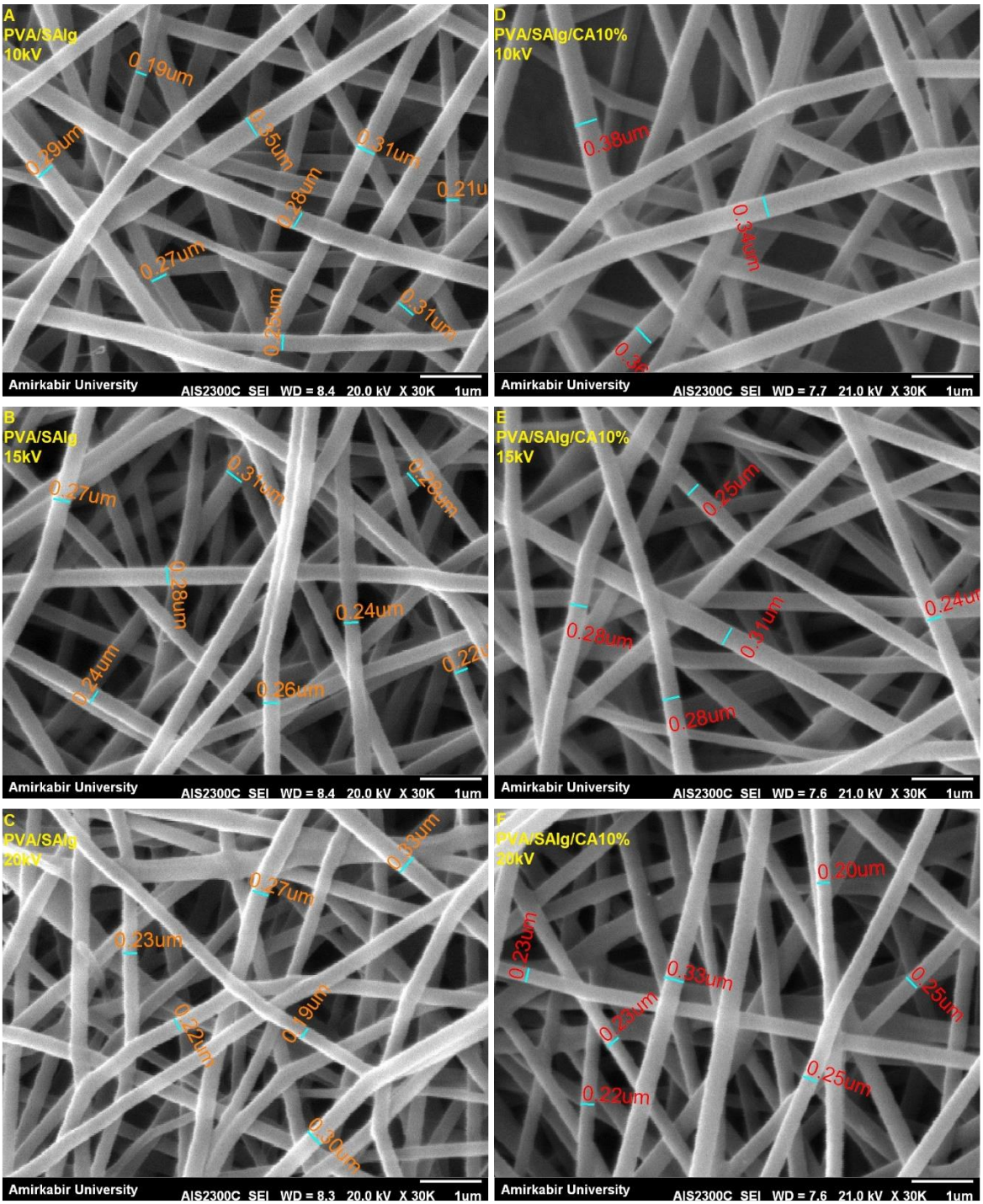

Figure1. SEM images of elctrospun PVA/SAlg and PVA/SAlg/CA10% mats nanofibers; With applied voltage of 10kV, 15kV, 20kV. (A) PVA/SAlg, 10kV; (B) PVA/SAlg, 15kV; (C) PVA/SAlg, 20kV; (D) PVA/SAlg/CA10%, 10kV; (E) PVA/SAlg/CA10%, 15kV; (F) PVA/SALg/CA10, 20kV

The morphology and the diameter distributions of the nanofibers are shown in Figures 2, 3, and 4. It seems that there is no drastic effect of increasing voltage on the morphology of nanofibers.

The scanning electron microscope images were processed by the image analysis software. The SEM images were classified into two-dimensional maps by the algorithm specified in the reference and

the histograms of the pore size distribution and diameter of the nanofibers were obtained from the maps. The used software was Image Version 1.8.

According to Table 1, the diameters of fibers change between 0.3893 to 0.4519 μm. The average diameter of electrospun PVA/SAlg was 0.4264, 0.3893, and 0.4046 μm at 10, 15, and 20 kV voltages, respectively. For PVA/SAlg/CA10% at the same voltages, were 0.4519, 0.4176, and 0.4375 μm. Initially decreased and then increased (Figures 2-5). The minimum diameter in both samples is observed at a voltage of 15 kV.

As seen in the table and figures, the mean diameter of the sample containing the drug at each voltage is greater than the diameter of the same sample without the drug at the same voltage; this can be due to the entrapment of the drug into the fibers and consequently an increase in diameter.

Table1. Different voltages and their effect on diameter, Pore size, and Porosity of PVA/SAlg and PVA/SAlg/CA10%

Sample	Diameter(μm)		Pore size (μm^2)	Porosity (%)
	Mean	SD		
PVA/SAlg, 5kV*	-	-	-	-
PVA/SAlg, 10kV	0.4264	0.1228	1.0275	43.56
PVA/SAlg, 15kV	0.3893	0.1244	0.9932	47.62
PVA/SAlg, 20V	0.4064	0.1407	0.8362	42.20
PVA/SAlg/CA10%, 5kV*	-	-	-	-
PVA/SAlg/CA10%, 10kV	0.4519	0.1237	1.1066	44.03
PVA/SAlg/CA10%, 15kV	0.4176	0.1226	1.0487	44.97
PVA/SAlg/CA10%, 20kV	0.4375	0.1372	1.0057	42.23

* No fiber deposition was seen from the solutions at the 5 kV

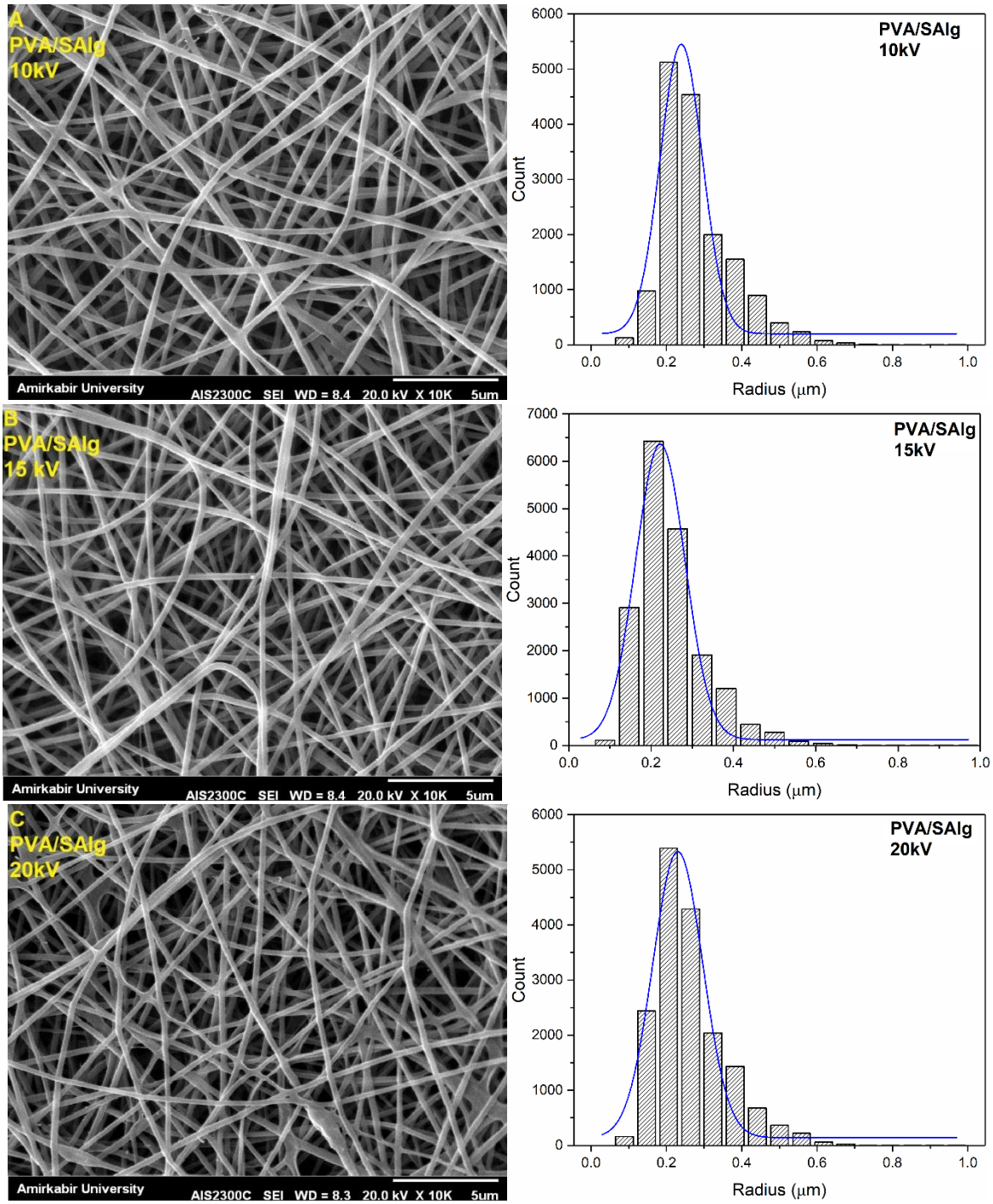

Figure2. SEM images and diameter distribution of the PVA/SAlg nanofiber mats with applied voltages, 10 kV: (A); 15 kV: (B); 20 kV: (C). Results are mean ± SD (n > 50)

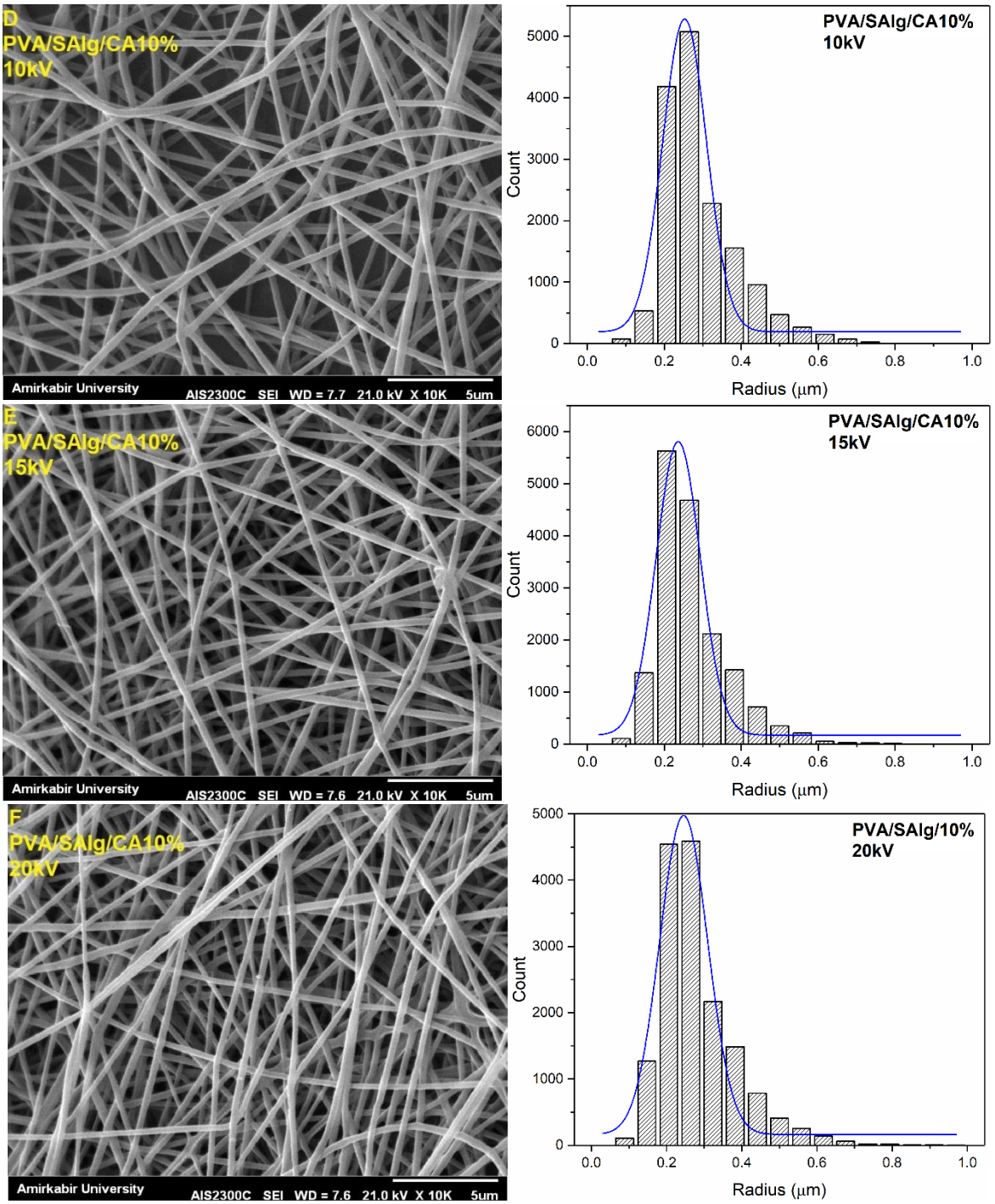

Figure3. SEM images and diameter distribution of the PVA/SAlg/CA10% nanofiber mats with applied voltages, 10 kV: (D); 15 kV: (E); 20 kV: (F). Results are mean ± SD (n > 50)

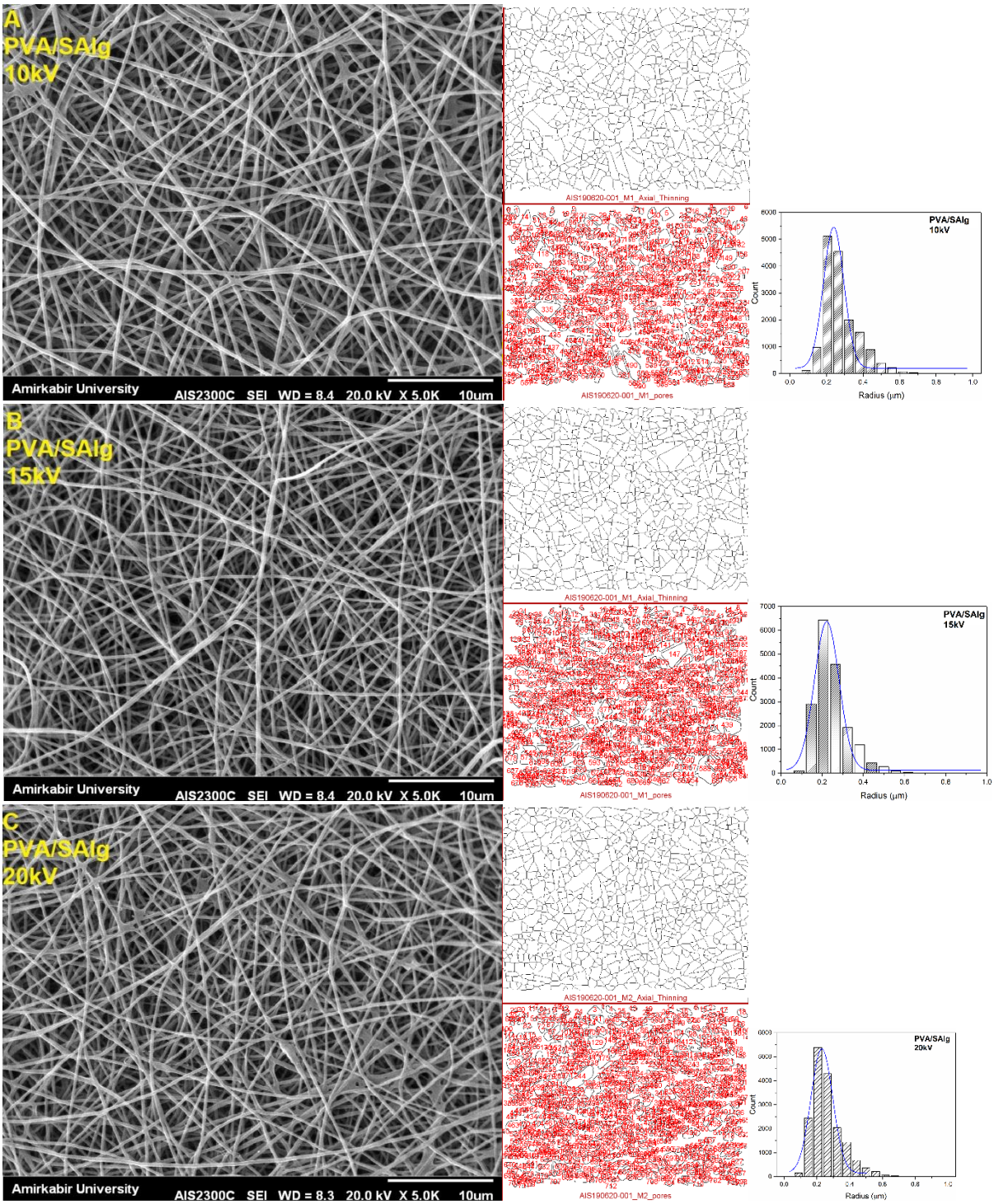

Figure4. SEM images and Radius(µm) distribution of the PVA/SAlg nanofiber mats with applied voltages Results are mean ± SD (n > 50) 10kV, (A); 15kV, (B); 20kV, (C)

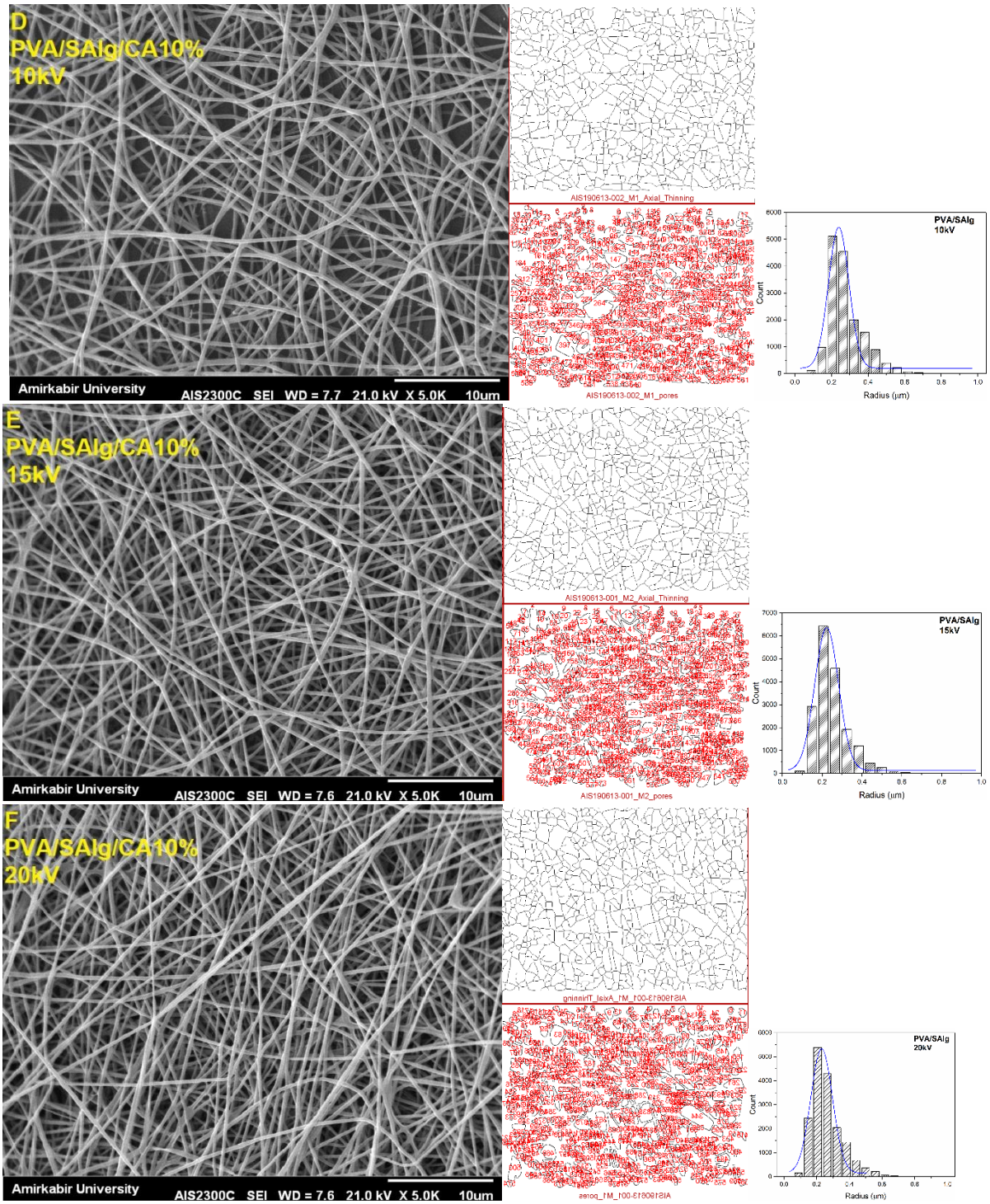

Figure5. SEM images and Radius(µm) distribution of the PVA/SAlg/CA10% nanofiber mats with applied voltages. Results are mean ± SD (n > 50) 10kV, (D); 15kV, (E); 20kV, (F)

Increasing the voltage thus brought about two opposite effects: (i) at first(Increasing the voltage from 10kV to 15kV) thinner fibers due to higher electric field strength, because the electrostatic force stretches the charged liquid to formation viscoelastic jets (ii) and then(Increasing the voltage from 15kV to 20kV) thicker fibers due to increased jet velocity, this causes the jet to hit the collector more quickly as well as the solvent has less time to evaporate and as a result their diameter

increases[26, 27]. In our study increasing the voltage from 10kV to 20 kV did not affect the electrospinning ability of the blend.

Nanofibrous mats pore size (1.0275, 0.9932 and 0.8362 μm2 in PVA/SAlg) and (1.1066, 1.0487 and 1.0057 μm2 in SAlg/PVA/CA10%) which are related to the 10, 15 and 20 kV voltages, respectively, decreased with the increment of voltage;

Nanofibrous mats porosity (43.56%, 47.62% and 42.20 % in PVA/SAlg) and (44.03%, 44.97% and 42.23% in PVA/SAlg/CA10%) which are related to the 10, 15 and 20 kV voltages, respectively, initially increased and then decreased with the increment of voltage (Unlike the changes in diameter that first decreased and then increased; (The maximum porosity in both samples is observed at a voltage of 15 kV).

It is observed that by reducing pore size, at first the porosity increases, but at 20 kV voltage again reduced, so that the minimum pore size and porosity are at this voltage (Table 1), (Figures 5).

The pore size of the sample containing the drug at each voltage is larger than the pore size of the same sample without the drug at the same voltage; This can be due to the larger diameter of the fibers in the samples containing the drug.

The porosity in drug-containing samples at each voltage is similar to that of drug-free samples.

Electrospinning process and the factors affecting properties of electrospun nanofibers have taken more attention from different fields lately. The applied voltage is one of the affecting parameters during electrospinning [26]. It is a general rule that a critical applied voltage is required for the electrospinning process to commence and a voltage lower than that would be insufficient to overcome the surface tension of the solution droplet. The critical or minimum voltage required for electrospinning to commence differs depending on the setup and solution used, with values typically greater than 4 kV, varying values of critical voltage from 4 kV to 19 kV in different solvent ratios. Increasing the applied voltage increases the electric field strength and repulsive forces on the fluid jet, favoring the formation of thinner fibers. However, the jet also tends to travel faster at a higher voltage, reducing the time taken for the thinning process, which can result in larger fiber diameters. Increasing the voltage thus brought about two opposite effects: (i) smaller fibers due to higher electric field strength and (ii) larger fibers due to increased jet velocity [27]. Morphology of electrospun nanofiber can be affected by the electrospinning device parameters including electric voltage, tip to collector distance, and solution parameters such as polymer concentration, feed mass ratio, and surface tension [28]. Changing the electric voltage could alter the fiber diameter and morphology [29], as shown in Figures 1 to 4. In a fixed flow rate of the electrospinning solution (0.5 mL / h), drum speed (500 rpm), and tip to collector distance (15 cm), it has been used 5, 10, 15, and 20 Kv applied voltage. In this study, the critical or minimum voltage required for electrospinning to commence was 8 kV.

4. Conclusion

Electrospinning was used to fabricate Nano-sized fibers based on PVA/SAlg and PVA /SAlg/CA10% blended aqueous solutions and were successfully electrospun to produce uniform fibers with a diameter range of 0.3893-0.4519 μm.

For both PVA/SAlg and PVA /SAlg/CA10%, the fiber diameter decreases as the applied voltage increases (other parameters constant), because, the jet diameter gets thinner and thinner as it

advances to the collector screen due to evaporation of the solvent and plastic deformation under the electrostatic forces. Increasing voltage accelerates the electrospinning jet and this may result in a greater volume of solution drawn from the tip of the needle, this results in a smaller and less stable Taylor cone, as a result, lead to greater stretching of the solution and this, in turn, should lead to thinner fibers; And then increase the voltage further leads to thicker fibers due to increased jet velocity, this causes the jet to hit the collector more quickly as well as the solvent has less time to evaporate and as a result their diameter increases.

In the PVA/SAlg/10%, the diameter of the fibers at each voltage is higher than the diameter of the fibers SAlg /PVA, this can be due to the loading of the drug (Calendula officinalis) into the fibers in PVA /SAlg/CA10%.

Finally, according to the findings of this study and the previous studies, the morphology of the PVA /SAlg mats (with the volume ratios of PVA to SAlg ranging 80/20) could be appropriate for the tissue engineering scaffold and the wound dressing, and drug loading causes a slight increase in diameter but does not cause a large change in the result. The results in this research showed that voltage of 15 kV is a good voltage for both PVA/SAlg and PVA /SAlg/CA10% to obtain uniform fibers and a relatively thinner diameter (Minimum diameter at this voltage relative to other voltages); On the other hand, the porosity is maximum at 15 kV in both samples (Both in the drug-containing sample and in the drug-free sample). These are especially important in wound dressing for proper vapor exchange. Given that the drug loading in the fibers increases fiber diameter, therefore, it is important to reach a suitable voltage that can modify this effect of increasing diameter. In tissue engineering, drug delivery systems, that require thinner or thicker fibers as well as the pore size and porosity symmetrical for the type of tissue studied in tissue engineering or drug release system and wound dressing, to bio-mimetic from native ECM, by increasing and decreasing the voltage (other parameters are constant), the diameter of the fibers, pore size and porosity can be reduced or increased to close the native ECM.

5. Acknowledgment

The authors would like to thank Ibn Masouyeh Pharmaceutical Company for providing Calendula Officinalis extract. We would like to thank the Stem Cell Technology Research Center facilities for assisting in electrospinning.

6. References

[1] Santos, C., Silva, C. J., Büttel, Z., Guimarães, R., Pereira, S. B., Tamagnini, P. and Zille, A. 2014. Preparation and Characterization of Polysaccharides/PVA Blend Nanofibrous Membranes by Electrospinning Method. Carbohydrate Polymers, 99: 584-592.

[2] Miguel, S. P., Figueira, D. R., Simões, D., Ribeiro, M. P., Coutinho, P., Ferreira, P. and Correia, I. J. 2018. Electrospun Polymeric Nanofibres as Wound Dressings: A review. Colloids and Surfaces B: Biointerfaces, 169: 60-71.

[3] Wang, M. and Zhao, Q. 2018. Electrospinning and Electrospray for Biomedical Applications. Reference Module in Biomedical Sciences: Encyclopedia of Biomedical Engineering. 1: 116-134.

[4] Alazab, M., Mitchell, G. R., Davis, F. J. and Mohan, S. D. 2017. Sustainable Electrospinning of Nanoscale Fibres. Procedia Manufacturing, 12: 66-78.

[5] Zamani, M., Prabhakaran, M. P. and Ramakrishna, S. 2013. Advances in Drug Delivery via Electrospun and Electrosprayed Nanomaterials. International journal of Nanomedicine. 8: 2997–3017.

[6] Bhardwaj, N. and Kundu, S. C. 2010. Electrospinning: A Fascinating Fiber Fabrication Technique. Biotechnology Advances. 28(3): 325-347.

[7] Boateng, J. and Catanzano, O. 2015. Advanced Therapeutic Dressings for Effective Wound Healing-A Review. Journal of Pharmaceutical Sciences. 104(11): 3653-3680.

[8] Draget, K. and Taylor, C. 2011. Chemical, Physical and Biological Properties of Alginates and their Biomedical Implications. Food Hydrocolloids - FOOD HYDROCOLLOID, 25: 251-256.

[9] Park, S.-B., Lih, E., Park, K.-S., Joung, Y. K., and Han, D. K. 2017. Biopolymer-based Functional Composites for Medical Applications. Progress in Polymer Science. 68: 77-105.

[10] Gutha, Y., Pathak, J. L., Zhang, W., Zhang, Y. and Jiao, X. 2017. Antibacterial and Wound Healing Properties of Chitosan/poly (Vinyl alcohol) /Zinc Oxide Beads (CS/PVA/ZnO). International Journal of Biological Macromolecules, 103: 234-241.

[11] Dutra, J. A., Carvalho, S., Zampirolli, A. C. D., Daltoé, R. D., Teixeira, R. M., Careta, F. and Konishi, J. 2016. Papain Wound Dressings Obtained from Poly (Vinyl alcohol) /Calcium Alginate Blends as New Pharmaceutical Dosage Form: Preparation and Preliminary Evaluation. European Journal of Pharmaceutics and Biopharmaceutics. 113: 11-23.

[12] Muppalaneni, S. 2013. Polyvinyl Alcohol in Medicine and Pharmacy: A Perspective. Journal of Developing Drugs. 2(3): 1-5.

[13] Gaaz, T. S., Sulong, A. B., Akhtar, M. N., Kadhum, A. A., Mohamad, A. B. and Al-Amiery, A. A. 2015. Properties and Applications of Polyvinyl Alcohol, Halloysite Nanotubes and Their Nanocomposites. Molecules (Basel, Switzerland). 20(12): 22833-22847.

[14] Yang, J. M., Yang, J. H., Tsou, S. C., Ding, C. H., Hsu, C. C., Yang, K. C. and Wang, J. S. 2016. Cell Proliferation on PVA/Sodium Alginate and PVA/Poly(γ-glutamic acid) Electrospun Fiber. Materials Science and Engineering: C. 66: 170-177.

[15] Shalumon, K. T., Haridas, A., Nair, S., Chennazhi, K. P. and Jayakumar, R. 2011. Sodium Alginate/poly(vinyl alcohol)/nano ZnO Composite Nanofibers for Antibacterial Wound Dressings. International Journal of Biological Macromolecules. 49: 247-254.

[16] Tang, Y., Xingzi, L., Liang, C., Zhong, Z., Xie, R., Zhou, Y. and Wang, W. 2019. Honey Loaded Alginate/PVA Nanofibrous Membrane as Potential Bioactive Wound Dressing. Carbohydrate Polymers. 219: 113-120.

[17] Kataria, K., Gupta, A., Rath, G., Mathur, R. B. and Dhakate, S. 2014. In Vivo Wound Healing Performance of Drug Loaded Electrospun Composite Nanofibers Transdermal Patch. International Journal of Pharmaceutics. 469: 102-110.

[18] Jarić, S., Kostić, O., Mataruga, Z., Pavlović, D., Pavlović, M., Mitrović, M. and Pavlović, P. 2018. Traditional Wound-healing Plants used in the Balkan Region (Southeast Europe). Journal of Ethnopharmacology. 211: 311-328.

[19] Kataria, K., Gupta, A., Rath, G., Mathur, R. B. and Dhakate, S. 2014. In Vivo Wound Healing Performance of Drug Loaded Electrospun Composite Nanofibers Transdermal Patch. International Journal of Pharmaceutics. 469: 102-110.

[20] Felgueiras, H. P. and Amorim, M. T. P. 2017. Functionalization of Electrospun Polymeric Wound Dressings with Antimicrobial Peptides. Colloids and Surfaces B: Biointerfaces. 156: 133-148.

[21] Islam, M. S. and Karim, M. 2010. Fabrication and Characterization of Poly(vinyl alcohol)/Alginate Blend Nanofibers by Electrospinning Method. Colloids and Surfaces A: Physicochemical and Engineering Aspects, 366(1-3), 135-140

[22] Safi, S., Morshed, M., Hosseini Ravandi, S. A. and Ghiaci, M. 2007. Study of Electrospinning of Sodium Alginate, Blended Solutions of Sodium Alginate/poly(viny1 alcoho1) and Sodium Alginate/poly(ethylene oxide). Journal of Applied Polymer Science. 104: 3245-3255.

[23] Wongkanya, R., Chuysinuan, P., Pengsuk, C. and Nooeaid, P. 2017. Electrospinning of Alginate/Soy Protein Isolated Nanofibers and Their Release Characteristics for Biomedical Applications. Journal of Science: Advanced Materials and Devices, 2(3): 309-316.

[24] Hotaling, N., Bharti, K., Kriel, H. and Simon, C. 2015. Dataset for the Validation and Use of DiameterJ an Open Source Nanofiber Diameter Measurement Tool. Data in brief. 5: 13-22.

[25] Quek, S. Y., Hadi, J. and Tanambell, H. 2018. Application of Electrospinning as Bioactive Delivery System. In Book: Reference Module in Food Science.

[26] Sener, A. G., Altay, A. S. and Lokumcu Altay, F. 2011. Effect of Voltage on Morphology of Electrospun Nanofibers. 7th International Conference on Electrical and Electronics Engineering (ELECO). 324-328.

[27] SalehHudin, H. S., Mohamad, E. N., Mahadi, W. N. L. and Muhammad Afifi, A. 2018. Multiple-jet Electrospinning Methods for Nanofiber Processing: A review. Materials and Manufacturing Processes. 33(5): 479-498.

[28] Liu, X., Yang, Y., Yu, D., Zhu, M.-J., Zhao, M. and Williams, G. 2018. Tunable Zero-order Drug Delivery Systems Created by Modified Triaxial Electrospinning. Chemical Engineering Journal. 356: 886-894.

[29] Long, Y.-Z., Yan, X., Wang, X.-X., Zhang, J. and Yu, M. 2019. Chapter 2 - Electrospinning: The Setup and Procedure. In B. Ding, X. Wang, & J. Yu (Eds.), Electrospinning: Nanofabrication and Applications (pp. 21-52): William Andrew Publishing.